MedChemComm

RSC Publishing

CONCISE ARTICLE

View Article Online
View Journal

Cite this: DOI: 10.1039/c3md00096f

Design and discovery of 4-anilinoquinazoline ureas as multikinase inhibitors targeting BRAF, VEGFR-2 and EGFR

Qingwen Zhang,*[a] Yuanyuan Diao,[a] Fei Wang,[b] Ying Fu,[a] Fei Tang,[a] Qidong You*[c] and Houyuan Zhou[a]

Received 28th March 2013
Accepted 26th April 2013

DOI: 10.1039/c3md00096f

www.rsc.org/medchemcomm

4-Anilinoquinazoline ureas were envisaged according to the hybrid-design approach based upon two privileged pharmacophores in kinase drug discovery, *i.e.* 4-anilinoquinazoline and unsymmetrical diaryl urea. In our structure–activity relationships (SAR) campaign, title compounds were synthesized and profiled in biochemical assay for their kinase inhibitory activity. Title compounds **18–20** were found to be multikinase inhibitors with profound activity against BRAF, BRAF V600E, VEGFR-2 and EGFR. Molecular docking into DFG-out conformations of BRAF and VEGFR-2 suggested that they might be type II inhibitors.

Introduction

Protein kinases have become the most important class of drug target in the field of oncology. Around 50–70% of current cancer drug discovery programs are focused on protein kinase inhibitors.[1] Since the launch of imatinib (Gleevec®) in 2001 for the treatment of patients with Philadelphia chromosome positive chronic myeloid leukemia (Ph + CML), some 20 small molecule protein kinase inhibitors have been approved for the targeted therapy of human cancers. A retrospective analysis of the chemical space explored by the medicinal chemistry efforts leading to these achievements found that 4-anilinoquinazoline and unsymmetrical diaryl urea are two privileged pharmacophores among others.[2,3] 4-Anilinoquinazoline is present in five launched products consisting of gefitinib (Iressa®), erlotinib (Tarceva®), lapatinib (Tykerb®), vandetanib (Caprelsa®), and icotinib (Conmana®). Unsymmetrical diaryl urea is present in two launched products, namely sorafenib (Nexavar®) and its fluoro congener regorafenib (Stivarga®) (Fig. 1).

Signalling pathways are not strictly linear processes but rather involve a complex network of interconnected circuits. When only a single pathway is targeted, redundancy and cross-talk between these pathways allow for compensatory effects by alternative pathways.[4] Thus, multikinase inhibition targeting the aberrant signalling network represents an important paradigm in targeted cancer drug discovery. The EGFR/Ras/RAF/MEK/ERK mitogen-activated protein kinase (MAPK) cascade is a key signalling pathway involved in the regulation of cell proliferation, survival and differentiation.[5] Aberrant activation of this pathway contributes to a wide range of human cancers.[5] In fact, BRAF was reported to be the most frequently mutated protein kinase in human cancers.[6] Meanwhile, VEGFR-2 has been proven to be the principal mediator in tumour angiogenesis, which is crucial for solid tumour development.[7] The successful launch of antiangiogenic drugs attests to the therapeutic value of VEGFR-2 inhibition.[8] Collectively, these facts justify the

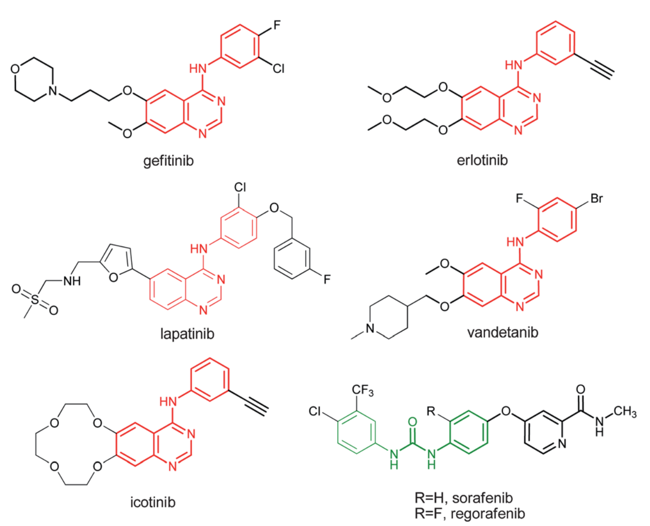

Fig. 1 Launched kinase inhibitors containing 4-anilinoquinazoline (shown in red) and unsymmetrical diaryl urea (shown in green) pharmacophores.

[a]Division of Medicinal Chemistry, Shanghai Institute of Pharmaceutical Industry, 1111 Zhongshan North One Road, Hongkou District, Shanghai 200437, China. E-mail: chembiomed@163.com; Fax: +86 (0)21 6516 9893; Tel: +86 (0)21 5551 4600

[b]State Key Laboratory of New Drug and Pharmaceutical Process, Shanghai Institute of Pharmaceutical Industry, 1111 Zhongshan North One Road, Hongkou District, Shanghai 200437, China

[c]Department of Medicinal Chemistry, School of Pharmacy, China Pharmaceutical University, 24 Tongjia Xiang, Nanjing, Jiangsu 210009, China. E-mail: youqd@163.com; Fax: +86 (0)25 8327 1351; Tel: +86 (0)25 8327 1351

development of multikinase inhibitors targeting BRAF, EGFR and VEGFR-2.

Sorafenib (BAY 43-9006) is an oral multikinase inhibitor approved by the U.S. Food and Drug Administration for the treatment of patients with advanced renal cell carcinoma (RCC) and patients with unresectable hepatocellular carcinoma (HCC). It was shown to be a dual action RAF kinase and VEGFR inhibitor targeting both the RAF/MEK/ERK pathway and receptor tyrosine kinases that promote angiogenesis.[9] Sorafenib is a type II inhibitor that stabilizes wild type BRAF and oncogenic mutant BRAF V600E as well as VEGFR-2 all in their inactive DFG-out conformations (PBD code 1UWH, 1UWJ and 4ASD, respectively).[10–13] Type II inhibitors may have some advantages including increased biochemical efficiency and the potential for achieving an increased degree of selectivity compared to type I inhibitors.[14] Thus, sorafenib was taken as a lead compound in our drug discovery endeavor to identify multikinase inhibitors targeting BRAF, EGFR and VEGFR-2.

According to the hybrid-design approach of rational design of inhibitors that bind to inactive kinase conformations, sorafenib is a first-generation type II inhibitor.[11] The binding affinity of sorafenib is mainly derived from a combination of hydrophobic and hydrogen bonding interactions of the biaryl urea portion ("tail") with the binding pocket created by the significant movement of the DFG motif. However, the binding affinity contributed by the 2-methylcarbamoylpyridinyl portion ("head") interacting with the hinge region is relatively small.

We reasoned that substituting 2-methylcarbamoylpyridinyl with a more efficient "head" portion might increase the overall binding affinity. 4-Anilinoquinazoline is a well-known type I scaffold that could deliver profound interactions with the kinase hinge residues and hydrophobic pockets in and around the adenine region.[11] Furthermore, 4-anilinoquinazoline is a well-known pharmacophore to deliver EGFR activity.[2] Hence, we employed 4-anilinoquinazoline as the "head" portion onto which the unsymmetrical diaryl urea "tail" was attached to give the novel hybrid scaffold (Fig. 2). This hybrid scaffold incorporates the two privileged pharmacophores into one single molecule. Furthermore, this hybrid scaffold fits the generalized pharmacophore model of type II inhibitors: the quinazoline hinge-binding moiety (HBM) is connected through a nitrogen atom to the central phenyl that is expected to occupy the DFG-out pocket (BPII). The central phenyl and the R^1 substituted terminal phenyl are linked by urea which functions as the hydrogen bond donor/acceptor to interact with the side chain of a conserved glutamic acid in the C helix and with the backbone amide of aspartic acid in the DFG motif. R^1 is expected to occupy the lipophilic pockets created by the displacement of the DFG loop (BPIII and BPIV).[10,15]

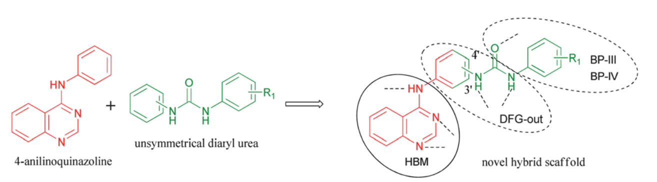

Fig. 2 Evolution of the novel hybrid scaffold based upon the two privileged pharmacophores 4-anilinoquinazoline (coloured in red) and unsymmetrical diaryl urea (coloured in green). Potential hydrogen bond interactions are depicted as dashed lines.

Results and discussion

Chemistry

Title compounds were prepared *via* the synthetic routes outlined in Scheme 1. 1-(4-Aminophenyl)-3-(4-chloro-3-(trifluoromethyl)phenyl)urea (**1**) was synthesized in a 10% yield by the reaction of isocyanate prepared *in situ* from 4-chloro-3-(trifluoromethyl)aniline with benzene-1,4-diamine. Compounds **5–7** were synthesized by nitro group reduction of compounds **2–4**, which were prepared in a one-pot procedure using triphosgene.[16,17]

Compound **8** was prepared from commercially available 3-hydroxy-4-methoxybenzaldehyde according to the literature.[18,19] Title compounds **9–12** were synthesized by condensation of **8** with **1** or **5–7** under acidic conditions in refluxing isopropanol.

Compounds **13** and **15** were prepared from 7-fluoroquinazolin-4(3*H*)-one, which was readily synthesized from commercially available 2-amino-4-fluorobenzoic acid according to the literature.[20–22] Compound **13** was condensed with **6** under acidic conditions in refluxing isopropanol to deliver title compound **14.** Compound **15** was condensed under acidic conditions in refluxing isopropanol with **5** and **6** to deliver intermediate compounds **16** and **17**, respectively. **16** and **17** were in turn reacted with aliphatic amine 2-(ethylamino)-ethanol or 2-(piperazin-1-yl)ethanol in the presence of potassium iodide in 1-methyl-2-pyrrolidinone (NMP) to give title compounds **18–20** (Scheme 1).

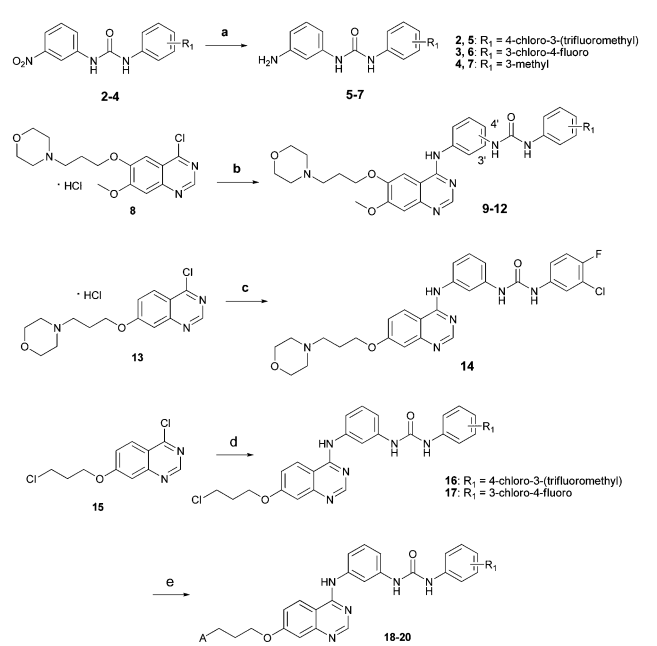

Scheme 1 *Reagents and conditions*: (a) Fe, NH_4Cl, EtOH–THF–H_2O, reflux, 83–94%; (b) **1** or **5–7**, HCl in i-PrOH, reflux, 11–61%; (c) **6**, HCl in i-PrOH, reflux, 11%; (d) **5** or **6**, HCl in i-PrOH, reflux, 60–75%; (e) 2-(ethylamino)ethanol or 2-(piperazin-1-yl)ethanol, KI, NMP, 50 °C, 20–82%.

Structure–activity relationships

The same quinazoline moiety seen in gefitinib was used in title compounds **9–12** (Table 1) to explore the structure–activity relationships (SAR) of the R_1-substituted urea moiety. **9–12** were tested for their inhibitory activity against BRAF, BRAF V600E, VEGFR-2 and EGFR. BRAF and BRAF V600E were tested in LanthaScreen format (http://www.invitrogen.com) according to the official protocol. VEGFR-2 and EGFR were tested in Caliper mobility shift assay format.[23]

Compound **9** was found to be 3-fold more active than sorafenib against VEGFR-2 (IC_{50} 17 nM), whilst displayed moderate activity against other 3 kinases. Compound **10** exhibited substantial activity against EGFR (IC_{50} 82 nM), whilst displayed moderate activity against VEGFR-2. The 4-anilinoquinazoline scaffold in **10** most likely contributes to the EGFR activity, since sorafenib is devoid of potency against EGFR. When compared with **9** having the 4′-urea linker, **10** having the 3′-urea linker exhibited 5- and 3-fold improvement in potency toward BRAF and BRAF V600E, respectively. This is consistent with SAR reported in the literature.[24] Substitution of 4-chloro-3-(trifluoromethyl)-phenyl for 3-chloro-4-fluorophenyl gave compound **11**, which proved to be nearly 4-fold more potent for BRAF and equipotent for BRAF V600E compared to sorafenib. However, compound **11** proved to be essentially inactive for VEGFR-2 and EGFR. Incorporation of 3-methylphenyl as the urea moiety (**12**) led to a slight improvement in potency toward BRAF and BRAF V600E but substantial loss of activity toward VEGFR-2 and EGFR when compared with **10**. Overall, 4-chloro-3-(trifluoromethyl)phenyl and 3-chloro-4-fluorophenyl attached at the 3′-position of the central phenyl seem to be the R_1-substituted urea moiety of choice.

In order to further explore SAR, elaboration of the C-7 substituent on the quinazoline ring was then undertaken. 4-Chloro-3-(trifluoromethyl)phenyl and 3-chloro-4-fluorophenyl attached at the 3′-position of the central phenyl were employed. The C-6 group was removed to allow a reduction in molecular weight and avoid any potential metabolic liability. Tethered aliphatic tertiary amino groups were ether-linked to C-7 of the quinazoline core to deliver target molecules **14** and **18–20** (Table 2).

Compound **14** exhibited superior activity against BRAF and comparable activity against BRAF V600E when compared with sorafenib. However, **14** exhibited only minimal activity for VEGFR-2 and EGFR. Incorporation of the more polar hydroxyl-bearing group 4-(hydroxyethyl)piperazin-1-yl or ethyl(2-hydroxyethyl)amino led to much improved potency toward VEGFR-2 and EGFR (**18–20**). Meanwhile, the activity toward BRAF and BRAF V600E was maintained (**18** and **19**) or even greatly improved (**20**). Compared to sorafenib, compound **20** was shown to be 5-fold more potent toward BRAF, and 3-fold more potent toward BRAF V600E. Thus, the hydroxyl-bearing title compounds **18–20** proved to be multikinase inhibitors with profound activity toward BRAF, BRAF V600E, VEGFR-2 and EGFR.

Overall, our 4-anilinoquinazoline urea scaffold seems to be a viable platform to deliver profound activity toward both threonine/serine kinases (BRAF and its oncogenic mutant BRAF V600E) and angiogenesis related receptor tyrosine kinases (VEGFR-2 and EGFR). Furthermore, it was observed that the potency for these kinases is governed by both the R_1-substituted urea moiety and the quinazoline C-7 side chain.

Molecular modeling

Molecular modeling was performed to establish the binding mode of selected title compounds. Docking of **20** in an X-ray crystal structure of sorafenib bound to BRAF (PDB code 1UWH) is depicted in Fig. 3(a).[12] **20** could be comfortably accommodated to the DFG-out conformation of BRAF. Quinazoline N1 accepts the hydrogen bond from the backbone amide NH of Cys531 in the hinge region. The quinazoline core is sandwiched by hydrophobic residues consisting of Ile462, Val470, Ala480, Trp530, Phe582 and Phe594, forming favorable π–π interaction (face-to-face) with the side chain of Trp530, and π–π interaction (face-to-edge) with the side chain of Phe594. The *meta*-disubstituted central phenyl linking to the quinazoline core through

Table 1 Kinase inhibitory activity (IC_{50}, nM) of title compounds **9–12**

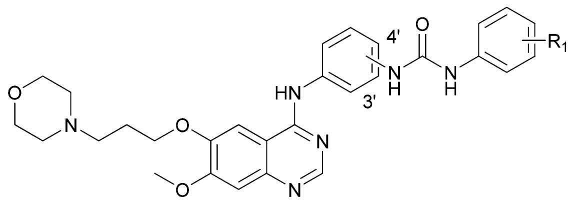

Compound	Position	R^1	R^2	BRAF[a]	BRAF V600E[a]	VEGFR-2[b]	EGFR[b]
9	4′	3-CF_3-4-Cl	H	539	371	17	285
10	3′	3-CF_3-4-Cl	H	195	75	213	82
11	3′	3-Cl-4-F	H	31	55	>10 000	>10 000
12	3′	3-CH_3	H	119	54	8568	2350
Sorafenib				114	42	52	>10 000

[a] Tested in LanthaScreen format. [b] Tested in Caliper mobility shift assay format.

Table 2 Kinase inhibitory activity (IC_{50}, nM) of title compounds **14** and **18–20**

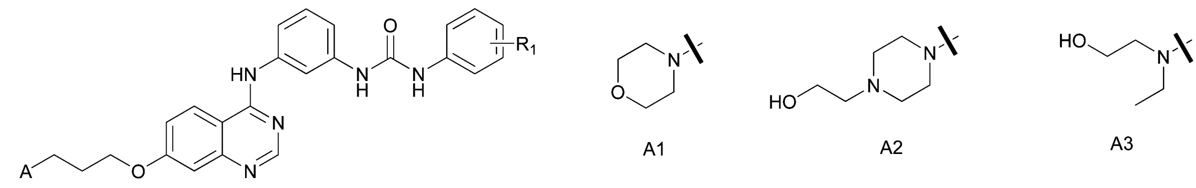

Compound	R[1]	A	BRAF[a]	BRAF V600E[a]	VEGFR-2[b]	EGFR[b]
14	3-Cl-4-F	A1	72	42	2165	3315
18	3-CF_3-4-Cl	A2	101	58	75	99
19	3-CF_3-4-Cl	A3	112	53	91	188
20	3-Cl-4-F	A3	22	13	95	165
Sorafenib			114	42	52	>10 000

[a] Tested in LanthaScreen format. [b] Tested in Caliper mobility shift assay format.

4-NH occupies the hydrophobic pocket neighboring the ATP binding site. Carbonyl and two NHs of urea form hydrogen bond interactions with the backbone of Asp593 and the side chain of Glu500, respectively. Terminal 4-chloro-3-(trifluoromethyl)phenyl extends into a second hydrophobic pocket produced by the movement of Phe594 and lined with Val503, Leu504, Ile512, Ile571 and His573.

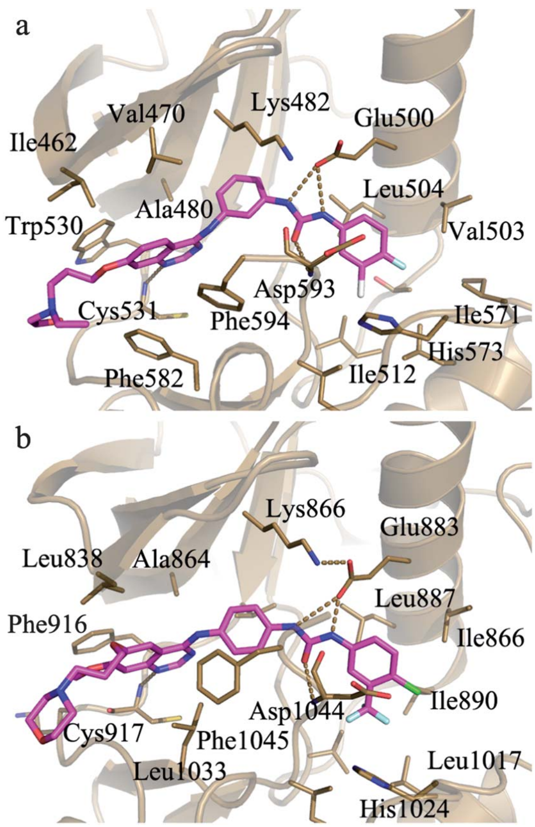

Fig. 3 (a) Molecular modeling of **20** (magenta) bound to BRAF. (b) Molecular modeling of **9** (magenta) bound to VEGFR-2. Hydrogen bonds are depicted as dashed grey lines. Key interacting residues are illustrated in brown sticks.

Docking of **9** in an X-ray cocrystal structure of VEGFR-2 (PDB code 2OH4) is depicted in Fig. 3(b).[25] Similar to the binding mode of **20** in BRAF, **9** could be comfortably accommodated to the DFG-out conformation of VEGFR-2. The quinazoline core is positioned in a hydrophobic cleft lined with Leu838, Ala864, Phe916 and Leu1033. Quinazoline N1 accepts the hydrogen bond from the backbone amide NH of Cys917 in the hinge region. The *para*-disubstituted central phenyl linking to the quinazoline core through 4-NH occupies the hydrophobic pocket neighboring the ATP binding site. Carbonyl and two NHs of urea form hydrogen bond interactions with the backbone of Asp1044 and the side chain of Glu883, respectively. Terminal 4-chloro-3-(trifluoromethyl)phenyl extends into a second hydrophobic pocket created by the flip of Phe1045 and lined with Ile866, Leu887, Ile890, Leu1017 and His1024.

Conclusion

In summary, we have described a hybrid-design approach based upon two privileged pharmacophores, namely 4-anilinoquinazoline and unsymmetrical diaryl urea, to successfully deliver a novel series of multikinase inhibitors. Title compounds **18–20** exhibited profound activity toward BRAF, BRAF V600E, VEGFR-2 and EGFR in biochemical screen. Molecular docking established the interactions of **20** and **9** with the DFG-out conformation of BRAF and VEGFR-2, respectively, suggesting that they might be type II kinase inhibitors. The SAR presented herein complemented by those independently reported by other scientists could give a more complete landscape in this field.[24,26–30] More work will have to be done to characterise the therapeutic relevance of this series of small molecules.

Experimental section

Chemistry

General methods. ^1H NMR was recorded on a Varian INOVA-400 400 MHz spectrometer. Chemical shifts (δ) are in ppm relative to the residual DMSO-d_6 signal (2.50 ppm), and coupling constants (J) are reported in Hz. The following abbreviations are used for multiplicities: s = singlet; br s = broad singlet; d = doublet; dd = double-doublet; t = triplet; m = multiplet. Mass spectra with electrospray ionization (MS-ESI) were recorded on a Waters Micromass Q-Tof micro instrument.

1-(4-Aminophenyl)-3-(4-chloro-3-(trifluoromethyl)phenyl)-urea (1). Triphosgene (1.19 g, 4 mmol) was dissolved in anhydrous methylene chloride (16 mL). Under nitrogen and ice-cooling, a mixture of 4-chloro-3-(trifluoromethyl)aniline (1.96 g, 10 mmol) and diisopropylethylamine (DIEA) (1.55 g, 12 mmol) in anhydrous methylene chloride was added slowly while maintaining the temperature of the reaction mixture at 25–35 °C. After a further 30 min of stirring, a mixture of benzene-1,4-diamine (1.08 g, 10 mmol) and DIEA (1.55 g, 12 mmol) in anhydrous methylene chloride was added in one portion. The resulting reaction mixture was stirred at room temperature for 24 h, and evaporated to dryness *in vacuo*. The residue was taken in ethyl acetate, washed consecutively with 10% aqueous potassium bisulfate, 5% aqueous sodium bicarbonate, and half-saturated brine, dried over anhydrous magnesium sulfate, and evaporated *in vacuo*. The residue was purified by basic Al_2O_3 column chromatography eluting with petroleum ether in EtOAc (60–0%) to give **1** as an off-white solid (0.34 g, 10%): ^{1}H NMR (DMSO-d_6) δ 8.91 (s, 1H, exchangeable), 8.23 (s, 1H, exchangeable), 8.07 (d, J = 2.4 Hz, 1H), 7.55–7.61 (m, 2H), 7.07 (d, J = 8.8 Hz, 2H), 6.53 (d, J = 8.8 Hz, 2H), 4.76 (s, 2H, exchangeable).

1-(3-Aminophenyl)-3-(4-chloro-3-(trifluoromethyl)phenyl)-urea (5). A suspension of **2** (ref. 17) (6.00 g, 16.7 mmol) in 95% ethanol (230 mL), THF (75 mL), and water (30 mL) was treated with iron powder (5.59 g, 100 mmol) (activated with 1 mol L^{-1} HCl before use) and ammonium chloride (0.89 g, 16.7 mmol). After being stirred under reflux for 1.5 h, the mixture was filtered through a pad of diatomaceous earth while still hot. The filtrate was concentrated. The concentrate was diluted with water and ethyl acetate, and the pH was adjusted to 9 with ammonium hydroxide. The aqueous phase was separated, and extracted with more ethyl acetate. The combined extracts were dried over anhydrous sodium sulfate, and concentrated to provide **5** as a pale yellow crystalline solid (5.15 g, 94%). ^{1}H NMR (DMSO-d_6) δ 8.97 (s, 1H, exchangeable), 8.44 (s, 1H, exchangeable), 8.11 (s, 1H), 7.58 (d, J = 1.6 Hz, 2H), 6.90 (t, J = 8.0 Hz, 1H), 6.80 (t, J = 2.0 Hz, 1H), 6.54–6.56 (m, 1H), 6.22–6.24 (m, 1H), 4.97 (s, 2H, exchangeable).

1-(3-Aminophenyl)-3-(3-chloro-4-fluorophenyl)urea (6). This compound was prepared from **3** (ref. 17) (10.22 g, 33 mmol) according to the procedure for **5** to afford **6** as an off-white crystalline solid (7.65 g, 83%). ^{1}H NMR (DMSO-d_6) δ 8.68 (s, 1H, exchangeable), 8.36 (s, 1H, exchangeable), 7.78 (dd, J = 2.0, 6.8 Hz, 1H), 7.28 (m, 2H), 6.90 (t, J = 8.0 Hz, 1H), 6.76 (s, 1H), 6.56 (d, J = 7.6 Hz, 1H), 6.22 (d, J = 7.6 Hz, 1H), 4.95 (s, 2H, exchangeable).

1-(3-Aminophenyl)-3-*m*-tolylurea (7). This compound was prepared from **4** (ref. 17) (1.71 g, 6.3 mmol) according to the procedure for **5** to afford **7** as an off-white solid (1.29 g, 85%). ^{1}H NMR (DMSO-d_6) δ 8.41 (s, 1H, exchangeable), 8.27 (s, 1H, exchangeable), 7.28 (s, 1H), 7.12–7.22 (m, 2H), 6.89 (t, J = 8.0 Hz, 1H), 6.77 (t, J = 2.0 Hz, 2H), 6.55 (dd, J = 1.2, 7.6 Hz, 1H), 6.20 (dd, J = 1.2, 8.0 Hz, 1H), 4.94 (s, 2H, exchangeable), 2.28 (s, 3H).

1-(4-Chloro-3-(trifluoromethyl)phenyl)-3-(4-(7-methoxy-6-(3-morpholinopropoxy)quinazolin-4-ylamino)phenyl)urea (9). A mixture of 4-(3-(4-chloro-7-methoxyquinazolin-6-yloxy)propyl) morpholine hydrochloride (**8**) (ref. 18 and 19) (0.37 g, 1.03 mmol), **1** (0.34 g, 1.03 mmol), isopropanol (10 mL) and saturated HCl solution in isopropanol (2.5 mL) was stirred under reflux for 3 h. After cooling to room temperature, the reaction mixture was diluted with methylene chloride (250 mL), methanol (50 mL) and water (50 mL). The resulting mixture was basified to pH 7.5 with 1 mol L^{-1} aqueous sodium hydroxide, and extracted with methylene chloride. The combined organic extract was washed with brine, dried over anhydrous sodium sulfate, and evaporated *in vacuo*. The resulting residue was purified by silica gel column chromatography eluting with EtOAc–EtOH–Et_3N 300 : 100 : 1 (v/v) to afford title compound **9** as an off-white solid (0.12 g, 18%). ^{1}H NMR (DMSO-d_6) δ 9.39 (s, 1H, exchangeable), 9.10 (s, 1H, exchangeable), 8.77 (s, 1H, exchangeable), 8.39 (s, 1H), 8.11 (d, J = 2 Hz, 1H), 7.82 (s, 1H), 7.61–7.68 (m, 4H), 7.47 (m, 2H), 7.16 (s, 1H), 4.19 (m, 2H), 3.92 (s, 3H), 3.57–3.59 (m, 4H), 2.46 (m, 2H), 2.40 (m, 4H), 1.99 (m, 2H). MS-ESI m/z 631 $(M + H)^+$.

1-(4-Chloro-3-(trifluoromethyl)phenyl)-3-(3-(7-methoxy-6-(3-morpholinopropoxy)quinazolin-4-ylamino)phenyl)urea (10). This compound was prepared from **8** (1.72 g, 4.6 mmol) and **5** (1.51 g, 4.6 mmol) according to the procedure for **9** to afford title compound **10** as a pale yellow solid (0.97 g, 61%). ^{1}H NMR (DMSO-d_6) δ 9.48 (s, 1H, exchangeable), 9.19 (s, 1H, exchangeable), 8.91 (s, 1H, exchangeable), 8.49 (s, 1H), 8.17 (d, J = 2.0 Hz, 1H), 8.02 (s, 1H), 7.92 (s, 1H), 7.63–7.66 (m, 2H), 7.52 (d, J = 8.4 Hz, 1H), 7.33 (t, J = 7.6 Hz, 1H), 7.23–7.24 (m, 2H), 4.26 (t, J = 6.4 Hz, 2H), 3.98 (s, 3H), 3.65 (m, 4H), 2.53 (m, 2H), 2.48 (m, 4H), 2.06 (m, 2H). MS-ESI m/z 631 $(M + H)^+$, 1261 $(2M + H)^+$.

1-(3-Chloro-4-fluorophenyl)-3-(3-(7-methoxy-6-(3-morpholinopropoxy)quinazolin-4-ylamino)phenyl)urea (11). This compound was prepared from **8** (1.41 g, 3.76 mmol) and **6** (1.12 g, 3.76 mmol) according to the procedure for **9** to afford title compound **11** as an off-white solid (0.15 g, 11%). ^{1}H NMR (DMSO-d_6) δ 9.44 (s, 1H, exchangeable), 8.82 (s, 1H, exchangeable), 8.77 (s, 1H, exchangeable), 8.47 (s, 1H), 7.82–7.98 (m, 3H), 7.21–7.47 (m, 6H), 4.23 (m, 2H), 3.96 (s, 3H), 3.61 (m, 4H), 2.52 (m, 2H), 2.43 (m, 4H), 2.02 (m, 2H). MS-ESI m/z 581 $(M + H)^+$, 603 $(M + Na)^+$, 1183 $(2M + Na)^+$.

1-(3-(7-Methoxy-6-(3-morpholinopropoxy)quinazolin-4-ylamino)phenyl)-3-*m*-tolylurea (12). This compound was prepared from **8** (0.45 g, 1.2 mmol) and **7** (0.29 g, 1.2 mmol) according to the procedure for **9** to afford title compound **12** as a pale yellow solid (0.21 g, 38%). ^{1}H NMR (DMSO-d_6) δ 9.42 (s, 1H, exchangeable), 8.66 (s, 1H, exchangeable), 8.54 (s, 1H, exchangeable), 8.45 (m, 1H), 7.96 (s, 1H), 7.88 (s, 1H), 7.43 (d, J = 7.6 Hz, 1H), 7.14–7.30 (m, 6H), 6.79 (d, J = 7.2 Hz, 1H), 4.22 (t, J = 6.4 Hz, 2H), 3.94 (s, 3H), 3.60 (m, 4H), 2.41 (m, 6H), 2.28 (s, 3H), 2.02 (m, 2H). MS-ESI m/z 543 $(M + H)^+$, 1085 $(2M + H)^+$.

1-(3-Chloro-4-fluorophenyl)-3-(3-(7-(3-morpholinopropoxy)-quinazolin-4-ylamino)phenyl)urea (14). A mixture of 4-(3-(4-chloroquinazolin-7-yloxy)propyl)morpholine hydrochloride (**13**) (ref. 21) (0.34 g, 1 mmol), **6** (0.35 g, 1.25 mmol), isopropanol

(8 mL) and saturated HCl solution in isopropanol (2 mL) was stirred under reflux for 4 h. After cooling to room temperature, the reaction mixture was evaporated *in vacuo*. The residue was diluted with water (10 mL), basified to pH 9 with 1 mol L^{-1} aqueous sodium hydroxide, and extracted with methylene chloride–methanol 3 : 1 (v/v) (3 × 60 mL). The combined organic extract was washed with water, dried over anhydrous sodium sulfate, and evaporated *in vacuo*. The resulting residue was purified by silica gel column chromatography eluting with EtOAc–EtOH–Et_3N 90 : 10 : 0.5 (v/v) to afford title compound **14** as a yellow solid (0.06 g, 11%). ^{1}H NMR (DMSO-d_6) δ 9.60 (s, 1H, exchangeable), 8.80 (s, 1H, exchangeable), 8.74 (s, 1H, exchangeable), 8.52 (s, 1H), 8.49 (d, J = 9.2 Hz, 1H), 7.99 (s, 1H), 7.81–7.82 (m, 1H), 7.49 (d, J = 8.0 Hz, 1H), 7.22–7.33 (m, 5H), 7.17 (d, J = 2.4 Hz, 1H), 4.20 (t, J = 6.4 Hz, 2H), 3.59 (m, 4H), 2.46–2.47 (m, 2H), 2.40 (t, J = 4.4 Hz, 4H), 1.95 (quintet, J = 6.8 Hz, 2H). MS-ESI m/z 601 $(M + H)^+$, 1201 $(2M + H)^+$.

1-(4-Chloro-3-(trifluoromethyl)phenyl)-3-(3-(7-(3-chloropropoxy)quinazolin-4-ylamino)phenyl)urea (16). A mixture of 4-chloro-7-(3-chloropropoxy)quinazoline (**15**) (ref. 22) (0.55 g, 2 mmol), **5** (0.66 g, 2 mmol), isopropanol (9 mL) and saturated HCl solution in isopropanol (2 mL) was stirred under reflux for 3 h. After cooling to room temperature, the reaction mixture was diluted with water, basified to pH 6–7 with 1 mol L^{-1} aqueous sodium hydroxide, and extracted consecutively with methylene chloride–methanol 1 : 3 (v/v) and methylene chloride. The combined organic extract was washed with brine, dried over anhydrous sodium sulfate, and evaporated *in vacuo*. The residue was crystallized from methanol to afford **16** as an off-white flake (0.83 g, 75%): ^{1}H NMR (DMSO-d_6) δ 10.87 (br s, 1H, exchangeable), 9.49 (s, 1H, exchangeable), 9.20 (s, 1H, exchangeable), 8.76 (s, 1H), 8.65 (d, J = 9.2 Hz, 1H), 8.14 (d, J = 1.6 Hz, 1H), 7.96 (s, 1H), 7.62 (m, 2H), 7.44 (dd, J = 2.4, 9.2 Hz, 2H), 7.36 (t, J = 8.0 Hz, 1H), 7.25–7.30 (m, 2H), 4.33 (t, J = 6.4 Hz, 2H), 3.85 (t, J = 6.4 Hz, 2H), 2.29 (dd, J = 6.4, 12.4 Hz, 2H). MS-ESI m/z 550 $(M + H)^+$, 1099 $(2M + H)^+$.

1-(3-Chloro-4-fluorophenyl)-3-(3-(7-(3-chloropropoxy)quinazolin-4-ylamino)phenyl)urea (17). This compound was prepared from **15** (0.26 g, 1 mmol) and **6** (0.28 g, 1 mmol) according to the procedure for **16** to afford **17** as an off-white solid (0.3 g, 60%). ^{1}H NMR (DMSO-d_6) δ 9.70 (br s, 1H, exchangeable), 8.84 (s, 1H, exchangeable), 8.76 (s, 1H, exchangeable), 8.55 (s, 1H), 8.52 (d, J = 9.2 Hz, 1H), 8.00 (s, 1H), 7.81–7.83 (m, 1H), 7.49 (d, J = 8.0 Hz, 1H), 7.20–7.36 (m, 6H), 4.30 (m, 2H), 3.87 (t, J = 6.8 Hz, 2H), 2.27 (m, 2H). MS-ESI m/z 500 $(M + H)^+$.

1-(4-Chloro-3-(trifluoromethyl)phenyl)-3-(3-(7-(3-(4-(2-hydroxyethyl)piperazin-1-yl)propoxy)quinazolin-4-ylamino)phenyl)urea (18). A mixture of **16** (0.15 g, 0.28 mmol), potassium iodide (0.09 g, 0.56 mmol), 2-(piperazin-1-yl)ethanol (0.15 g, 1.12 mmol) and NMP (2 mL) was heated to 50 °C for 32 hours with protection from light. After cooling to room temperature, the reaction mixture was purified directly on silica gel eluting with EtOAc–EtOH–Et_3N from 300 : 100 : 1.5 to 100 : 100 : 1.5 (v/v), and finally recrystallized from MeOH–EtOAc 6 : 1 (v/v) to give title compound **18** as a pale yellow solid (0.07 g, 39%). ^{1}H NMR (DMSO-d_6) δ 11.40 (br s, 1H, exchangeable), 9.81 (s, 1H, exchangeable), 9.54 (s, 1H, exchangeable), 8.86 (s, 1H), 8.74 (d, J = 8.8 Hz, 1H), 8.15 (s, 1H), 7.93 (s, 1H), 7.60 (dd, J = 8.8,22.4 Hz, 2H), 7.49 (d, J = 9.2 Hz, 1H), 7.33–7.41 (m, 4H), 4.34 (m, 2H), 3.66–3.81 (m, 10H), 3.40 (m, 2H), 3.33 (m, 2H), 2.30 (m, 2H). MS-ESI m/z 644 $(M + H)^+$.

1-(4-Chloro-3-(trifluoromethyl)phenyl)-3-(3-(7-(3-(ethyl(2-hydroxyethyl)amino)propoxy)quinazolin-4-ylamino)phenyl) urea (19). This compound was prepared from **16** (0.15 g, 0.28 mmol) and 2-(ethylamino)ethanol (0.10 g, 1.12 mmol) according to the procedure for **18** to afford title compound **19** as a pale yellow powder (0.14 g, 82%). ^{1}H NMR (DMSO-d_6) δ 9.73 (s, 1H, exchangeable), 9.20 (s, 1H, exchangeable), 8.91 (s, 1H, exchangeable), 8.55 (s, 1H), 8.53 (d, J = 9.2 Hz, 1H), 8.14 (s, 1H), 8.02 (s, 1H), 7.61 (m, 2H), 7.53 (d, J = 8.4 Hz, 1H), 7.19–7.32 (m, 4H), 5.32 (br s, 1H, exchangeable), 4.27 (t, J = 6.4 Hz, 2H), 3.77 (m, 2H), 3.30 (m, 2H), 3.21 (m, 4H), 2.21 (t, J = 7.2 Hz, 2H), 1.26 (t, J = 7.2 Hz, 3H). MS-ESI m/z 603 $(M + H)^+$.

1-(3-Chloro-4-fluorophenyl)-3-(3-(7-(3-(ethyl(2-hydroxyethyl)-amino)propoxy)quinazolin-4-ylamino)phenyl)urea (20). This compound was prepared from **17** (0.14 g, 0.28 mmol) and 2-(ethylamino)ethanol (0.10 g, 1.12 mmol) according to the procedure for **18** to afford title compound **20** as a white solid (0.03 g, 20%). ^{1}H NMR (DMSO-d_6) δ 9.65 (s, 1H, exchangeable), 8.91 (s, 1H, exchangeable), 8.82 (s, 1H, exchangeable), 8.50–8.53 (m, 2H), 8.00 (s, 1H), 7.80–7.82 (m, 1H), 7.50 (d, J = 8.4 Hz, 1H), 7.19–7.35 (m, 6H), 5.30 (br s, 1H, exchangeable), 4.27 (t, J = 5.6 Hz, 2H), 3.76 (m, 2H), 3.20–3.29 (m, 6H), 2.20 (m, 2H), 1.25 (t, J = 6.8 Hz, 3H). MS-ESI m/z 553 $(M + H)^+$, 1105 $(2M + H)^+$.

Biology

Materials. BRAF, BRAF V600E, LanthaScreen Tb-anti-pMAP2K1 [pS217/221] Ab, Fluorescein-MAP2K1 (inactive) and Antibody Dilution Buffer were purchased from Invitrogen. EGFR and VEGFR-2 were purchased from Carna. ATP, DMSO, EDTA, GW5074 and staurosporine were purchased from Sigma. 96-well plate and 384-well plate were purchased from Corning.

LanthaScreen kinase assay

A LanthaScreen kinase assay (http://www.invitrogen.com) was used to measure the potency of title compounds against BRAF and BRAF V600E. GW-5074 was used as the reference compound. Compounds were prepared in DMSO at 10 mM and serially diluted in a 96-well plate as the source plate. 4 μL was transferred to a new 96-well plate as the intermediate plate, and mixed with 96 μL of 1× kinase buffer (50 mM HEPES, pH 7.5; 10 mM $MgCl_2$; 1 mM EGTA; 0.01% Brij-35). 2.5 μL was transferred to a 384-well assay plate in duplicate. 5 μL of BRAF 7 nM or BRAF V600E 0.7 nM, 2.5 μL of substrate solution containing Fluorescein-MAP2K1 0.8 μM and ATP (for BRAF 2 μM, for BRAF V600E 6 μM) were added to the assay plate and incubated with the compound for 1 hour at room temperature. The reaction was stopped with the addition of 10 μL of detection solution (antibody 4 nM and EDTA 20 mM in Antibody Dilution Buffer) to each well of the assay plate. After mixing briefly with a centrifuge and incubating for at least 30 minutes, the plate was read on a Victor instrument (Ex. 340 nm, Em. 520 nm). RFU values from the Victor program were converted to percent inhibition values according to percent inhibition = (max-sample RFU)/(max − min) × 100%, in which "max" means the RFU of no enzyme control and "min" means the RFU of DMSO control. Plots of percent inhibition *versus* compound concentration were fitted by Graphpad 5.0 to calculate IC_{50} of test compounds.

Caliper motility shift assay

A Caliper motility shift assay was used to measure the potency of title compounds against VEGFR-2 and EGFR. Compounds were prepared in DMSO at 10 mM and serially diluted in 96-well plates to obtain 5× compound solution in 10% DMSO of 10 concentrations ranging from 50 μM to 2.5 nM. 50 μL of 10% DMSO was transferred for DMSO control. 70 μL of 250 mM EDTA was transferred for low control. Staurosporine was used as the reference compound.

Kinase reaction: Add 10 μL of kinase (VEGFR-2 4.5 nM or EGFR 20 nM) into 1.25× kinase base buffer (62.5 mM HEPES, pH 7.5; 0.001875% Brij-35; 12.5 mM $MgCl_2$; without (VEGFR-2) or with (EGFR) 12.5 mM $MnCl_2$; 2.5 mM DTT) to prepare 2.5× enzyme solution. Transfer 5 μL of each 5× compound solution in 10% DMSO to the 384-well assay plate in duplicate. Transfer 10 μL of 2.5× enzyme solution to each well of the 384-well assay plate. Incubate at room temperature for 10 min. Transfer 10 μL of 2.5× peptide solution (prepared by adding FAM-labeled peptide and ATP (VEGFR-2 230 μM or EGFR 5.75 μM) into the 1.25× kinase base buffer) to each well of the 384-well assay plate. Incubate at 28 °C for 1 h. Add 25 μL of stop buffer (100 mM HEPES, pH 7.5; 0.015% Brij-35; 0.2% Coating Reagent #3; 50 mM EDTA) to stop the reaction.

Collect conversion data on Caliper EZ Reader II. Convert conversion values to inhibition values according to percent inhibition = (max-conversion)/(max − min) × 100%, in which "max" stands for DMSO control, "min" stands for low control. Fit the data in XLfit to obtain IC_{50} values. The equation used is

$$Y = \text{Bottom} + (\text{Top} - \text{Bottom})/(1 + 10\text{^}((\log IC_{50} - X) \times \text{HillSlope})).$$

Molecular modeling

Docking was carried out using AutoDock 4. X-ray cocrystal structures of BRAF (PDB code 1UWH) and VEGFR-2 (PDB code 2OH4) were downloaded from RCSB Protein Data Bank and prepared using AutoDockTools 1.4. Water molecules and small inorganic ions were removed. Default parameters in AutoDock 4 were used in this study.

Acknowledgements

We are grateful to the Basic Research Key Program of Shanghai Municipal (no. 09JC1413200) and the National Science and Technology Major Project "Key New Drug Research and Development" (no. 2009ZX09301-007) for financial support. We thank Shanghai ChemPartner Co., Ltd. (Pudong New Area, Shanghai 201203, China) for generating kinase inhibitory data.

References

1 P. Cohen and D. R. Alessi, *ACS Chem. Biol.*, 2012, **8**, 96–104.
2 A. J. Bridges, *Chem. Rev.*, 2001, **101**, 2541–2571.
3 J. Dumas, R. A. Smith and T. B. Lowinger, *Curr. Opin. Drug Discovery Dev.*, 2004, **7**, 600–616.
4 R. Morphy, *J. Med. Chem.*, 2010, **53**, 1413–1437.
5 P. J. Roberts and C. J. Der, *Oncogene*, 2007, **26**, 3291–3310.
6 C. Greenman, P. Stephens, R. Smith, G. L. Dalgliesh, C. Hunter, G. Bignell, H. Davies, J. Teague, A. Butler, C. Stevens, S. Edkins, S. O'Meara, I. Vastrik, E. E. Schmidt, T. Avis, S. Barthorpe, G. Bhamra, G. Buck, B. Choudhury, J. Clements, J. Cole, E. Dicks, S. Forbes, K. Gray, K. Halliday, R. Harrison, K. Hills, J. Hinton, A. Jenkinson, D. Jones, A. Menzies, T. Mironenko, J. Perry, K. Raine, D. Richardson, R. Shepherd, A. Small, C. Tofts, J. Varian, T. Webb, S. West, S. Widaa, A. Yates, D. P. Cahill, D. N. Louis, P. Goldstraw, A. G. Nicholson, F. Brasseur, L. Looijenga, B. L. Weber, Y.-E. Chiew, A. deFazio, M. F. Greaves, A. R. Green, P. Campbell, E. Birney, D. F. Easton, G. Chenevix-Trench, M.-H. Tan, S. K. Khoo, B. T. Teh, S. T. Yuen, S. Y. Leung, R. Wooster, P. A. Futreal and M. R. Stratton, *Nature*, 2007, **446**, 153–158.
7 K. Holmes, O. L. Roberts, A. M. Thomas and M. J. Cross, *Cell. Signalling*, 2007, **19**, 2003–2012.
8 F. Musumeci, M. Radi, C. Brullo and S. Schenone, *J. Med. Chem.*, 2012, **55**, 10797–10822.
9 S. M. Wilhelm, C. Carter, L. Y. Tang, D. Wilkie, A. McNabola, H. Rong, C. Chen, X. M. Zhang, P. Vincent, M. McHugh, Y. C. Cao, J. Shujath, S. Gawlak, D. Eveleigh, B. Rowley, L. Liu, L. Adnane, M. Lynch, D. Auclair, I. Taylor, R. Gedrich, A. Voznesensky, B. Riedl, L. E. Post, G. Bollag and P. A. Trail, *Cancer Res.*, 2004, **64**, 7099–7109.
10 J. J. L. Liao, *J. Med. Chem.*, 2007, **50**, 409–424.
11 Y. Liu and N. S. Gray, *Nat. Chem. Biol.*, 2006, **2**, 358–364.
12 P. T. C. Wan, M. J. Garnett, S. M. Roe, S. Lee, D. Niculescu-Duvaz, V. M. Good, C. M. Jones, C. J. Marshall, C. J. Springer, D. Barford and R. Marais, *Cell*, 2004, **116**, 855–867.
13 M. McTigue, B. W. Murray, J. H. Chen, Y.-L. Deng, J. Solowiej and R. S. Kania, *Proc. Natl. Acad. Sci. U. S. A.*, 2012, **109**, 18281–18289.
14 F. Lovering, J. McDonald, G. A. Whitlock, P. A. Glossop, C. Phillips, A. Bent, Y. Sabnis, M. Ryan, L. Fitz, J. Lee, J. S. Chang, S. Han, R. Kurumbail and A. Thorarensen, *Chem. Biol. Drug Des.*, 2012, **80**, 657–664.
15 D. Niculescu-Duvaz, C. Gaulon, H. P. Dijkstra, I. Niculescu-Duvaz, A. Zambon, D. Menard, B. Suijkerbuijk, A. Nourry, L. Davies, H. Manne, F. Friedlos, L. Ogilvie, D. Hedley, S. Whittaker, R. Kirk, A. Gill, R. D. Taylor, F. I. Raynaud, J. Moreno-Farre, R. Marais and C. J. Springer, *J. Med. Chem.*, 2009, **52**, 2255–2264.
16 P. Majer and R. S. Randad, *J. Org. Chem.*, 1994, **59**, 1937–1938.
17 Q. Zhang, Q. You, H. Zhou and D. Yuanyuan, *Zhongguo Yiyao Gongye Zazhi*, 2012, **43**, 247–250.

18 Y. Diao and Q. Zhang, *Zhongguo Yiyao Gongye Zazhi*, 2008, **39**, 401–403.
19 J. P. Gilday and D. Moody, WO pat. 2004024703 A1, 2004.
20 L. F. Hennequin, A. P. Thomas, C. Johnstone, E. S. E. Stokes, P. A. Ple, J. J. M. Lohmann, D. J. Ogilvie, M. Dukes, S. R. Wedge, J. O. Curwen, J. Kendrew and C. Lambert-van der Brempt, *J. Med. Chem.*, 1999, **42**, 5369–5389.
21 A. P. Thomas, C. Johnstone and L. F. Hennequin, U. S. pat. 6291455 B1, 2001.
22 A. A. Mortlock, K. M. Foote, N. M. Heron, F. H. Jung, G. Pasquet, J. J. M. Lohmann, N. Warin, F. Renaud, C. De Savi, N. J. Roberts, T. Johnson, C. B. Dousson, G. B. Hill, D. Perkins, G. Hatter, R. W. Wilkinson, S. R. Wedge, S. P. Heaton, R. Odedra, N. J. Keen, C. Crafter, E. Brown, K. Thompson, S. Brightwell, L. Khatri, M. C. Brady, S. Kearney, D. McKillop, S. Rhead, T. Parry and S. Green, *J. Med. Chem.*, 2007, **50**, 2213–2224.
23 A. Card, C. Caldwell, H. Min, B. Lokchander, H. Xi, S. Sciabola, A. V. Kamath, S. L. Clugston, W. R. Tschantz, L. Wang and D. J. Moshinsky, *J. Biomol. Screening*, 2009, **14**, 31–42.
24 M. W. Holladay, B. T. Campbell, M. W. Rowbottom, Q. Chao, K. G. Sprankle, A. G. Lai, S. Abraham, E. Setti, R. Faraoni, L. Tran, R. C. Armstrong, R. N. Gunawardane, M. F. Gardner, M. D. Cramer, D. Gitnick, M. A. Ator, B. D. Dorsey, B. R. Ruggeri, M. Williams, S. S. Bhagwat and J. James, *Bioorg. Med. Chem. Lett.*, 2011, **21**, 5342–5346.
25 M. Hasegawa, N. Nishigaki, Y. Washio, K. Kano, P. A. Harris, H. Sato, I. Mori, R. I. West, M. Shibahara, H. Toyoda, L. Wang, R. T. Nolte, J. M. Veal and M. Cheung, *J. Med. Chem.*, 2007, **50**, 4453–4470.
26 A. Garofalo, L. Goossens, A. Lemoine, A. Farce, Y. Arlot and P. Depreux, *J. Enzyme Inhib. Med. Chem.*, 2010, **25**, 158–171.
27 A. Garofalo, L. Goossens, A. Lemoine, S. Ravez, P. Six, M. Howsam, A. Farce and P. Depreux, *Med. Chem. Commun.*, 2011, **2**, 65–72.
28 A. Garofalo, L. Goossens, P. Six, A. Lemoine, S. Ravez, A. Farce and P. Depreux, *Bioorg. Med. Chem. Lett.*, 2011, **21**, 2106–2112.
29 A. Garofalo, L. Goossens, B. Baldeyrou, A. l. Lemoine, S. v. Ravez, P. Six, M.-H. l. n. David-Cordonnier, J.-P. Bonte, P. Depreux, A. l. Lansiaux and J.-F. o. Goossens, *J. Med. Chem.*, 2010, **53**, 8089–8103.
30 A. Garofalo, A. Farce, S. Ravez, A. Lemoine, P. Six, P. Chavatte, L. Goossens and P. Depreux, *J. Med. Chem.*, 2012, **55**, 1189–1204.

